# Portable LCD Image Quality: Effects of Surround Luminance

Youn Jin Kim
*Samsung Electronics Company, Ltd.*
*Korea*

## 1. Introduction

Liquid crystal display (LCD) has become a major technology in a variety of display application markets from small sized portable displays to large sized televisions. Portable LCD devices such as smart phones and mobile phones are used in a diverse range of viewing conditions. We usually experience images on a mobile phone with a huge loss in contrast under bright outdoor viewing conditions; thus, viewing condition parameters such as surround effects, correlated colour temperature and ambient lighting have become of significant importance. (Katoh et al., 1998; Moroney et al., 2002) Recently, auxiliary attributes determining the mobile imaging were examined and the surround luminance and ambient illumination effects were considered as the first major factor. (Li et al., 2008) Surround and ambient lighting effects on colour appearance modelling have been extensively studied to understand the nature of colour perception under various ambient illumination levels (Liu & Fairchild, 2004, 2007; Choi et al., 2007; Park et al., 2007); thus, this study intends to figure out characteristics of the human visual system (HVS) in *spatial frequency domain* by means of analysing the contrast discrimination ability of HVS. In consequence, we propose an image quality evaluation method and a robust image enhancement filter based on the measured contrast sensitivity data of human observers under various surround luminance levels.

The former is to quantify the observed trend between surround luminance and contrast sensitivity and to propose an image quality evaluation method that is adaptive to both surround luminance and spatial frequency of a given stimulus. The non-linear behaviour of the HVS was taken into account by using contrast sensitivity function (CSF). This model can be defined as the square root integration of multiplication between display modulation transfer function (MTF) and CSF. It is assumed that image quality can be determined by considering the MTF of an imaging system and the CSF of human observers. The CSF term in the original SQRI model (Barten, 1990) is replaced by the surround adaptive CSF quantified in this study and it is divided by the Fourier transform of a given stimulus.

The latter is a robust image enhancement filter which compensates for the effects of surround luminance on our contrast perceiving mechanism. Precisely, the surround luminance adaptive CSF is used as a guide for determination of the adaptive enhancement gain in the proposed algorithm.

## 2. Measuring and modelling of the surround adaptive CSF

This study examined the effects of surround luminance on shape of spatial luminance CSF and reduction in brightness of uniform neutral patches shown on a computer controlled display screen is also assessed to explain the change of CSF shape. Consequently, a large amount of reduction in contrast sensitivity at middle spatial frequencies can be observed; however, the reduction is relatively small for low spatial frequencies. In general, effect of surround luminance on the CSF appears the same to that of mean luminance. Reduced CSF responses result in less power of the filtered image; therefore, the stimulus should appear dimmer with a higher surround luminance.

### 2.1 Backgrounds

The CSF represents the amount of minimum contrast at each spatial frequency that is necessary for a visual system to distinguish a sinusoidal grating or Gabor patterns over a range of spatial frequencies from a uniform field. Physiologically, both parvocellular (P) and magnocellular (M) cells have receptive fields organised into two concentric antagonistic regions: a centre (on- or off-) and a surrounding region of opposite sense. This arrangement is common in vertebrates. The receptive fields of small bistratified cells appear to lack clear centre-surround organization. (Dacey & Lee, 1994) The distributions of sensitivity within centre and surround mechanisms are usually represented by Gaussian profiles of a ganglion cell's receptive field. The spatial properties of the visual neurons are commonly inferred from a neuron's spatial modulation transfer function (van Nes & Bouman, 1967) or contrast sensitivity function (Enroth-Cugell & Robson, 1966) measured with grating patterns whose luminance is modulated sinusoidally. In practice, monochromatic patterns in which luminance varies sinusoidally in space are used. CSFs typically plot the reciprocal of the minimum contrast that is also referred to as threshold and provide a measure of the spatial properties of contrast-detecting elements in the visual system. (Campbell and Green, 1965) It is believed that CSF is in fact the envelope of the sensitivity functions for collections of neural channels that subserve the detection and discrimination of spatial patterns. (Braddick et al., 1978; Graham, 1980)

The first measurement of luminance CSF for the human visual system (HVS) was reported by Schade (Schade, 1956) in 1956 and the luminance CSF has been extensively studied over a variety of research fields - such as optics, physiology, psychology, vision and colour science - and the same basic trends were observed. Luminance CSF exhibits a peak in contrast sensitivity at moderate spatial frequencies (~ 5.0 cycles per degree; cpd) (Campbell & Green, 1965) and falls off at both lower and higher frequencies; thus, generally shows band-pass characteristics. The fall-off in contrast sensitivity at higher spatial frequency can be explained by spatial limitations in the retinal mosaic of cone receptors. The reduction in contrast sensitivity at lower spatial frequencies requires further neural explanations. (Westland et al., 2006) Centre-surround receptive fields are one possible reason for this low-frequency fall-off. (Wandell, 1995)

CIE technical committee (TC) 1-60 (Martinez-Uriegas, 2006) has recently collected luminance CSF measurement data from various literatures. (Campbell & Robson, 1968; Watson, 2000; Martinez-Uriegas et al., 1995; Barten, 1999) Those data were measured using different experimental contexts; for instance, Campbell and Robson used Garbor patches and the others used sinusoidal gratings. The all data were normalised to unity at the maximum contrast sensitivity of each data set for a cross-comparison on a single plot. Consequently,

they corresponded to one another and their trends are remarkably similar; therefore, they could be accurately fit by a single CSF model (Barten, 1999) in spite of the significant difference in conditions, methods and stimulus parameters.

The CSF model used was originally proposed by Barten as a function of spatial frequency and dependent on a field size (or viewing angle in degree) and mean luminance of the sinusoidal grating stimulus. As the mean luminance of the sinusoidal grating stimulus is decreased, the following variations occur (See Fig. 1). The contrast sensitivity at each spatial frequency decreases, and the maximum resolvable spatial frequency decreases. In addition, the shape of luminance CSF changes; the peaks in the functions shift toward lower spatial frequencies, broaden, and eventually disappear. (Rohaly & Buchsbaum, 1989; Patel, 1966; de Valois et al., 1974)
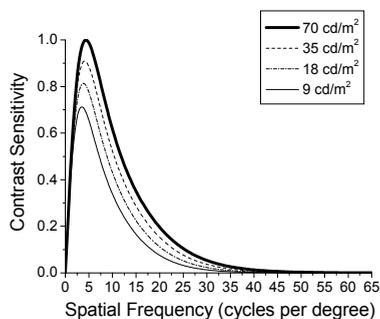


Fig. 1. Predicted CSF by Barten's model with various mean luminance levels for a field size of 5 degrees. As the mean luminance of the sinusoidal grating stimulus is decreased, contrast sensitivity at each spatial frequency decreases, and the maximum resolvable spatial frequency decreases as well. The peaks in the functions shift toward lower spatial frequencies and broaden.

The wealth of data in the literature also reports a variety of changes in CSF shape with senescence, (Owsley et al., 1983; Tulunay-Keesey et al., 1988; Higgins et al., 1988; Rohaly & Owsley, 1993; Pardhan, 2004) eccentricity (Rovamo et al., 1978; Koenderink et al., 1979; Wright & Johnston, 1983; Johnston, 1987; Snodderly et al., 1992) and degree of adaptation to noise (Farchild & Johnson, 2007) in a given stimulus. Briefly, luminance CSFs for older subjects exhibit losses in contrast sensitivity at the higher frequencies, although much of the loss is attributed to optical factors. (Owsley et al., 1983; Burton et al., 1993) Sensitivity to the local contrast at the peripheral region can be measured by instructing the observer to fixate on a marker whilst the actual object is placed at some distance from the marker. The distance is usually expressed in an angular measure called 'eccentricity' and the contrast sensitivity is measured as a function of eccentricity. With increasing eccentricity, capillary coverage increases up to 40%. (Snodderly et al., 1992) Fairchild and Johnson (Farchild & Johnson, 2007) found the fact that the adapted luminance CSF relates to the reciprocal of the adapting stimulus' spatial frequency. However, surround effects on the luminance CSF in spatial frequency domain appears to be less well investigated so far. Cox et al. (Cox et al., 1999) measured the effect of surround luminance on CSF and visual acuity using computer-generated sinusoidal gratings under a surround levels up to 90 cd/m² for the purpose of

ophthalmic practice in 1999. In consequence, reduced contrast sensitivity was measured under the highest surround luminance (90 cd/m²) and the optimal surround level was found to be at 10 ~ 30% of mean luminance of a target stimulus. Precisely, contrast sensitivity increases when luminance of the surround increases from 0 to 10 ~ 20% of that of stimulus; however once the surround luminance exceeds the optimal level contrast sensitivity suddenly falls off.

Recently, portable display devices such as mobile phones and portable media players are viewed in a diverse range of surround luminance levels and we usually experience images on a mobile phone display with a huge loss in contrast under bright outdoor viewing conditions. Ambient illumination and surround have been thought of as the first major factor among the mobile environmental considerations (Li et al., 2008); therefore, it is worthy to measure the changes in luminance CSF shape under highly bright surrounds as a simulation of outdoor sunlight. In two psychophysical experiments we examined luminance CSFs under different surround luminance levels are estimated and change in brightness of uniform neutral patches shown on a computer controlled display screen is observed. In specific, Experiment 1 is conducted to measure the compound results of contrast threshold perception and physical contrast of a display resulted from the increase of ambient illumination. The former could be attributed to simultaneous lightness contrast (Palmer, 1993) between stimuli on a display and surround luminance so may cause change in CSF. The latter is usually decreased by the surface light reflections off the front of the monitor screen referred to as viewing flare. In addition, a more psychophysics for variation in brightness is carried out to support and justify the surround effects in Experiment 2.

In this study, MTF of the display used is computed for each surround condition and divides the results from Experiment 1 in order to deduct the display's resolution term as well as effects of viewing flare. Because resolution of the display device used may limit the detectable contrast sensitivity of a human observer, the display factor should be discounted. In an equation form, let $F(u, v)$ represent MTF of a display which comes from the Fourier transformed line spread function (LSF). If the image from the display is filtered by CSF denoted by $H(u, v)$, the Fourier transform of the output $\psi(u, v)$ can be given by (Barten, 1990, 1999)

$$\psi(u,v) = H(u,v)F(u,v) \tag{1}$$

where $u$ and $v$ are spatial frequency variables.

Therefore, CSF $H(u, v)$ can be estimated by deducting MTF $F(u, v)$ in linear system (See eq. (2)). Viewing flare is an additional luminance across the whole tonal levels from black to white and increases the zero frequency response only. More detailed discussions are followed in Results section.

$$H(u,v) = \psi(u,v)/F(u,v) \tag{2}$$

## 2.2 Methods
### 2.2.1 Apparatus
A 22.2-inc. Eizo ColorEdge221 liquid crystal display (LCD) was used to present experimental stimuli such as sinusoidal gratings and uniform neutral patches. Spatial resolution of the LCD is 1920 × 1200 pixels and the bit depth was 8 bits per channel. The maximum luminance producible is approximately 140 cd/m² in a dark room and the black

level elevates up to 1 cd/m² due to the inherent leakage light problem of typical LCDs. The display was illuminated by using an EVL lighting colourchanger 250 light source in a diagonal direction. The ambient illuminance levels could be adjusted by changing the distance between the display and light source. Two particular illuminance levels, i.e. 7000 and 32000 lx, were achieved when the distance settings from the display are respectively 270 and 135 cm. The white coloured wall located behind the display was used as surround. In our previous works, (Kim et al., 2007, 2008) illuminance of few real outdoor viewing situations was measured. The lower level (7000 lx) is for simulating 'overcast' and the higher one (32000 lx) for 'bright' outdoor sunlight conditions. Note that the light source illuminates not only the surround region but also the display screen. The physical contrast loss, which can be caused by the light reflection from the screen (See Table 1), is deducted by using MTF of the display for each viewing condition. More details about this viewing flare compensation will be discussed later in Results section.

|  | Dark | Overcast | Bright |
|---|---|---|---|
| $L_{max}$ (cd/m²) | 140 | 147 | 154 |
| $L_{min}$ (cd/m²) | 1 | 8 | 15 |
| Viewing Flare (cd/m²) | 0 | 7 | 14 |
| Michelson Contrast (Mc) | 0.986 | 0.897 | 0.828 |
| Relative Mc to Dark | 1 | 0.910 | 0.840 |
| Surround luminance (cd/m²) | 0 | 1500 | 7000 |

Table 1. Breakdown of each viewing condition

Table 1 provides measured maximum and minimum luminance levels of the display for each viewing condition along with the viewing flare, absolute Michelson contrast (Mc), relative Mc to dark and surround luminance. Viewing flare can be estimated by the additional luminance increase due to the ambient illumination. As surround is changed from dark to overcast to bright, mean of evenly sampled 8 luminance values across the surround wall behind the display increases from 0 to 1500 to 7000 cd/m². The amount of viewing flare also increases, so Michelson contrast levels (See eq. (3)) are respectively decreased to 0.897 and 0.822 for overcast and bright as given in Table 1.

$$Michelson\ Contrast = (L_{max} - L_{min}) / (L_{max} + L_{min}) \qquad (3)$$

where $L$ is luminance and maxima and minima are taken over the vertical position of the sinusoidal grating stimulus pattern.

The temporal stability of the light source was measured every 20 seconds continuously for 30 minutes from the cold start and the results are depicted in Fig. 2. Crosses are measured data points for overcast and open circles are for bright. The illuminance level became stable after approximately 3 minutes for both cases. The stabilised illuminance values for the two lighting conditions were fluctuating around 6000 ~ 8000 lx for overcast and 31000 ~ 37000 lx for bright and their mean could be found near 7000 and 32000 lx.

### 2.2.2 Experiment 1: Compound results of contrast threshold perception and physical contrast variation

Experiment 1 is conducted to measure compound results of contrast threshold perception and physical contrast reduction caused by increase of ambient illumination. The former is
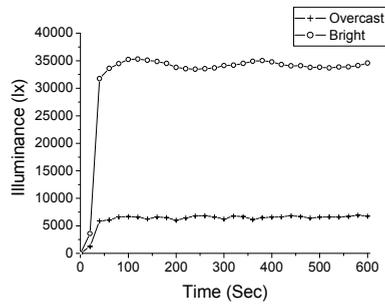
Fig. 2. Temporal illuminance measurement of the simulated outdoor sunlight using EVL lighting colourchanger 250. The temporal stability of the light source was measured every 20 seconds continuously for 30 minutes from the cold start. Crosses are measured data points for overcast and open circles are for bright. The illuminance level became stable after approximately 3 minutes for both cases.

affected by the level of surround luminance and the latter relates to the amount of viewing flare that was provided in Table 1. A sinusoidal grating pattern, of which contrast modulation gradually varies, is displayed on the display. Along the vertical axis of the screen, contrast becomes the highest in the bottom and lowest in the top of the pattern as can be seen in Fig. 3. This sinusoidal grating pattern (**Q**) was produced by means of the product of a non-linear gradient function along the vertical axis (**M**) and a one-dimensional sinusoidal function of spatial frequency across the horizontal axis (**F**). Practically, those functions can be discretely sampled and expressed by

$$\mathbf{Q} = \mathbf{MF}^\mathrm{T} \tag{4}$$

where $\mathbf{F}^\mathrm{T}$ denotes transpose of $\mathbf{F}$.

The compound effects of contrast threshold perception and physical contrast were measured at 11 spatial frequencies: 1, 2, 3, 4, 5, 6, 7, 13, 23, 32 and 65 cpd. The first 7 spatial frequencies (1 to 7 cpd) are sampled at the low spatial frequency area with steps of 1 cpd in order to accurately measure the peak sensitivity and the sharp fall-off of CSF. Two middle spatial frequencies, 13 and 23 cpd, where the gradual fall-off after the peak can be observed, are also selected. The highest spatial frequency sampled in this study is 65 cpd for predicting the maximum resolvable frequency.



Fig. 3. Example of sinusoidal grating stimulus. Along the vertical axis of the screen, contrast becomes the highest in the bottom and lowest in the top of the pattern.

In total, 6 observers (4 females and 2 males) participated in Experiment 1 and their ages ranged from 26 to 38. They were required to identify vertical positions of the sinusoidal pattern, by double-clicking a wireless mouse, when the contrast becomes just indistinguishable. This experimental technique emulates a method suggested by (Kitaguchi & MacDonald, 2006). We implemented a software using Microsoft foundation class in Visual C++ 6.0 to display sinusoidal patterns, to read the coordinates of double-clicked vertical position by the observer and to calculate the contrast. Technically, contrast can be defined as Michelson contrast (See eq. (3)) and it is usually converted into sensitivity unit that is the reciprocal of contrast threshold as given in eq. (5).

$$Sensitivity = 1 \ / \ Threshold \qquad\qquad (5)$$

Each sinusoidal pattern is displayed on the LCD monitor in a random order. Under the dark surround condition, the procedure was repeated for 5 times and the results were averaged to obtain contrast threshold values. The same procedure was also applied for the other viewing conditions: overcast and bright. The sequence of these psychophysical sessions for the viewing conditions was also randomly decided for each observer. In order to assure maximum observer adaptation to the viewing condition including the LCD monitor white point and ambient illumination level, observers were given 30 seconds adaptation period (Fairchild & Reniff, 1995) prior to each session. Precisely, observers were instructed to stare at a full white patch displayed on the LCD monitor screen under a certain ambient illumination. The distance between an observer and LCD was set to be 3 m in order to minimize the quantization error of the 8-bit display used. The total number of psychophysical assessments collected for data analysis was 990 (11 stimuli × 5 repeats × 6 observers × 3 viewing conditions).

### 2.2.3 Experiment 2: Magnitude estimation of brightness

Experiment 2 aims to measure the change in brightness (Blakeslee et al., 2008) of a series of neutral colours shown on an LCD under varied ambient illumination levels and to find out whether the brightness change can affect the contrast threshold perception of human observers. The brightness / lightness distinction may not always be clear to subjects. (Arend & Spehar, 1993a, 1993b; Rudd & Popa, 2007) Lightness means perceived reflectance as a surface property, while brightness is even more ambiguously defined as the perceived luminance of a light source or subjective correlate of luminance. (Rudd & Popa, 2007) We decided to adopt brightness because the all test stimuli used are shown on a monitor rather than reflective colours.

Nine neutral patches were uniformly sampled across a 8-bit RGB scale from 0 to 255 with steps of 51 and each of the neutral colours was displayed at a time on the whole LCD screen. Five observers (2 females and 3 males) participated in this experiment in total and their ages ranged from 26 to 38. The apparent brightness of a full white patch displayed on the LCD monitor screen of which the RGB values are (255, 255, 255) was assigned as an arbitrary brightness magnitude value of 100. Prior to the brightness estimations, observers were required to memorize the white patch on the monitor in a dark room and judge a brightness ratio of each of the rest of test neutral colours at a time not only under dark but also under the other two ambient illumination conditions: overcast and bright. Observers were given the following written-instruction. "*Please estimate the level of perceived brightness according to the reference patch of which its perceived brightness is assigned as 100.*" Each observer repeated all

judgments five times in a random order and its mean opinion score (MOS) (ITU-R, 2002) was collected for data analysis.

The sequence of the experiment for those ambient illumination conditions was also randomly decided for each observer and a mid-gray of which RGB value is (128, 128, 128) was shown to the observer as a transient patch whilst changing stimulus. The transient patch is usually displayed to prevent from any illusions while the scene is changed. In the field of image quality, this illusion artefact is referred to as image sticking. (Lee et al., 2009) In order to assure maximum observer adaptation to the viewing condition including the LCD monitor white point and ambient illumination level, observers were given the 30 seconds adaptation period (Fairchild & Reniff, 1995) prior to each session. They were allowed to look back into the reference white patch under dark viewing condition but re-adaptations were performed when viewing condition is altered. The total number of psychophysical assessments used for data analysis was 675 (9 stimuli × 5 repeats × 5 observers × 3 viewing conditions).

### 2.2.4 Experiment 3: Statistical analysis for observer variation

Variation between observers was evaluated in terms of three test methods: ITU-R BT 500-10, a modified version of coefficient of variance (CV) (Luo et al., 1991) and the Pearson correlation. First, ITU-R BT 500-10 method (ITU-R, 2002) rejects observations which are statistically incoherent with the other observers and show unusual peakedness of the probability distribution of a real-valued random variable. It should be ascertained whether the distribution of an observer's data is normal, using the Kurtosis test. Second, CV is often used as a measure of the 'observer accuracy' which represents the mean discrepancy of a set of psychophysical data obtained from a panel of observers from their mean value. This term has been widely used in colour appearance and difference studies (Luo et al., 2001, 2006) and usage of it was also verified in image quality studies. (Kim et al., 2008, 2010a, 2010b) The original CV is a normalised measure of dispersion for a repeated measurement but was applied to measure the degree to which a set of data points varies in this study. The CV is normally displayed as percentage and, for a perfect agreement between them, equals to 0. Third, Pearson correlation reflects the degree of linearity in the relationship between a pair of variables (e.g. $x$ and $y$). It is defined to be the sum of the products of the standard score of the two variables divided by the degree of freedom. When the variables are perfectly linearly related, their Pearson correlation is +1.

### 2.3 Results
### 2.3.1 Observer variation

Performance of the observers participated in Experiments 1 and 2 was evaluated using the three statistical test methods previously introduced and so obtained results are summarised in Table 2. Basically, the all observations can be accepted by ITU-R BT 500-10 method and CV values ranged from 19 to 25 in Experiment 1 which can be within the acceptable level for observer accuracy. (Kim et al., 2008, 2010a, 2010b; Luo et al., 2006) Even lower CV values were measured in Experiment 2 (13 ~ 18) because of the simplicity of magnitude estimation technique. Pearson correlations for the all assessments are larger than 0.98 meaning the strong linearity between the mean and each observation. Especially for Experiment 2, since brightness estimates are known for their subject variability, the individual data are also illustrated along with their mean for each viewing condition in later section.

| Experiment | Method | Dark | Overcast | Bright |
|---|---|---|---|---|
| 1 | ITU-R BT 500-10 | All passed | All passed | All passed |
| | CV | 20 | 19 | 25 |
| | r | 0.983 | 0.996 | 0.994 |
| 2 | ITU-R BT 500-10 | All passed | All passed | All passed |
| | CV | 13 | 18 | 17 |
| | r | 0.993 | 0.994 | 0.991 |

Table 2. Observer variation test results

### 2.3.2 Compound results of contrast threshold perception and physical contrast

In Experiment 1, the compound results of contrast threshold perception and physical contrast loss were achieved. They resulted from the increase of ambient illumination level causing both increase of surround luminance and viewing flare. The measured data were converted into the sensitivity unit using eq. (5), which is denoted as *psi* ($\psi$), in eqs. (1) through (2). Figure 4 depicts those $\psi$ data for the three viewing conditions. Every data point was normalised to the unity at the maximum value obtained in dark (288) and adjacent data are linearly connected. Consequently, as the viewing condition changes from dark to overcast to bright, the data moved toward zero in general. The shape of the all three plots appears typical band-pass and the spatial frequency where the maximum contrast sensitivity occurred was moved toward a lower frequency, i.e. from 5 to 4 cpd. The compound effects of surround luminance and viewing flare on the contrast threshold perception and physical contrast loss seem to be similar to that of mean luminance as previously reported by the wealth of data in the literature as discussed in Introduction section. Error bars represent standard errors that can be defined as standard deviation divided by square root of number of observations.

### 2.3.3 Deriving the display MTF

It is often assumed that the point spread function (PSF) of a majority of commercial LCD monitors is a rectangle function, *rect(x)*, (Barten, 1991; Sun & Fairchild, 2004) because the shape of a single pixel in LCDs is rectangular as illustrated in Fig. 5 (a). The rectangle function can be defined as

$$rect(x) = 1 \qquad \text{if} \qquad |x| \le n/2$$

otherwise

$$rect(x) = 0 \tag{6}$$

where *n* is the size of a pixel of an LCD in visual angle. (Sun & Fairchild, 2004)

Magnitude of the Fourier transform of the rectangle function can be expressed as shown in eq. (7).

$$MTF(u) = \left| \Im \left[ rect(x) \right] \right|$$
$$= \left| \frac{\sin \pi n u}{\pi u} \right| \tag{7}$$

(a) Dark
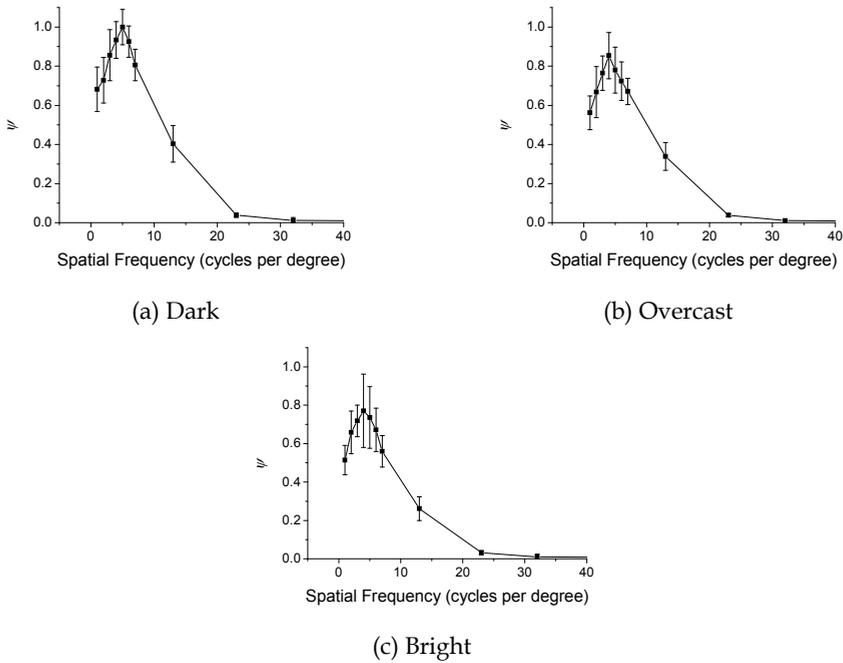


(b) Overcast



(c) Bright

Fig. 4. Measured data from Experiment 1 under 3 different ambient illumination conditions with linear interpolation for (a) dark (b) overcast and (c) bright. As the viewing condition changes from dark to overcast to bright, the data moved toward zero in general. The shape of the plots appears typical band-pass and the spatial frequency where the maximum contrast sensitivity occurred was moved toward a lower frequency, i.e. from 5 to 4 cpd.



(a)



(b)
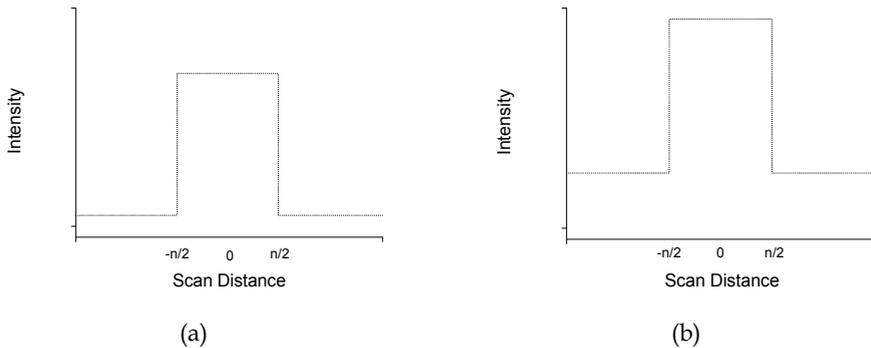
Fig. 5. (a) The original PSF and (b) viewing flare added PSF. Viewing flare is an additional luminance across the whole tonal levels from black to white and increases the zero frequency response only.

Then eq. (7) is divided by $n$, because $MTF(u)$ should equal to 1, so sinc function can be used as the MTF of LCDs.

$$MTF(u) = \left| \frac{\sin \pi n u}{\pi n u} \right|$$

$$= \left| \sin c \left( \pi n u \right) \right| \tag{8}$$

where $\Im[\cdot]$ denotes the Fourier transform of the argument.

Viewing flare can be defined as the additional luminance due to surface reflections off the front of a display caused by ambient illumination. It boosts the PSF by a constant offset level as illustrated in Fig. 5 (b); thus, the zero frequency response (or *dc* component) is increased only and other frequency responses remain the same if the signal is transformed into Fourier domain. When the MTF is normalised at the maximum, $MTF(0) = 1$ and $MTF(u>0)$ is multiplied by a weighting factor $a$ for $u > 0$ as shown in eq. (9).

$$MTF_i(u) = \alpha MTF_0(u)$$

$$= \alpha \left| \sin c \left( \pi n u \right) \right| \tag{9}$$

where $i$ represents the amount of viewing flare. For instance of this, $MTF_0$ shows the MTF for dark viewing condition so $MTF_i$ is the MTF for a viewing condition where the amount of viewing flare is $i$ cd/m². The weighting factor $a$ refers to the ratio of zero frequency response between $MTF_0(u)$ and $MTF_i(u)$ as given in Eq. (10). Practically, mean value of the PSF can be simply used instead of calculating zero frequency response of the MTF in Fourier domain therefore $a$ values should be identical to the relative Michelson contrast to the dark viewing condition as can be expected (See Table 1).

$$\alpha = \frac{MTF_0(0)}{MTF_i(0)} = \frac{\left( L_{Max,0} + L_{Min,0} \right) / 2}{\left( L_{Max,i} + L_{Min,i} \right) / 2} \tag{10}$$

The estimated MTF of the LCD monitor used in this study is presented in Fig. 6 (See the solid line). Single-pixel size of the LCD is set to be 0.00474° in visual angle unit. The estimated MTFs for the higher illumination levels are shown in Fig. 6 as well represented by dashed and dotted lines.
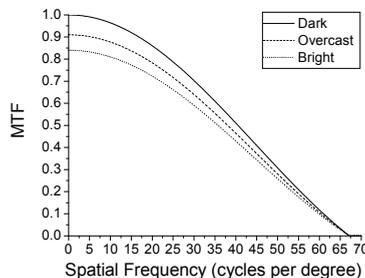


Fig. 6. MTF of the LCD used in this study and the approximated MTFs under two different levels of viewing flare. Single-pixel size of the LCD is set to be 0.00474° in visual angle unit. The compensation factors (*a*) for viewing flare for the three viewing conditions are listed in Table 3.

|       | Dark | Overcast | Bright |
|-------|------|----------|--------|
| $\varphi$ | 1    | 0.534    | 0.191  |

Table 3. The surround luminance effect function ($\varphi$)

### 2.3.4 Estimating CSF by compensating for MTF

As given in eqs. (1) through 2 in Introduction section, CSFs for the three viewing conditions can be estimated by dividing $\psi$ measured in Experiment 1 by the corresponding MTFs as illustrated in Fig. 7. Data points for dark are linearly interpolated and represented by solid lines and dashed lines for overcast and dotted lines for bright. As can be seen, they show band-pass characteristics and the peak contrast sensitivity for dark is observed at 5 cpd but it moves to 4 cpd for overcast and bright. The peak-shift appears more obvious compared to Fig. 4. However, it is not quite easy to yield significance of the shift on the sampling frequency of 1 cpd. A large amount of reduction in contrast sensitivity at middle frequency area ($4 < u < 13$) can be observed; however, little reduction in contrast sensitivity is found for lower frequencies ($u < 4$). Because the MTF converges to zero at near the maximum spatial frequency we sampled (68 cpd) so contrast sensitivity at 65 cpd is not investigated in the current section due to the limited display resolution.
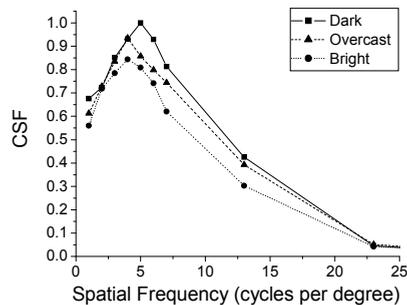


Fig. 7. Estimated CSF data points under 3 different surround luminance levels with linear interpolation. The all three plots show band-pass characteristics and the peak spatial frequency for dark is 5 cpd but moves to 4 cpd for overcast and bright. A large amount of reduction in contrast sensitivity at middle frequency area ($4 < u < 13$) can be observed; however, little reduction in contrast sensitivity is found for lower frequencies ($u < 4$).

Figure 8 illustrates the ratio of the area covered by the three linearly interpolated plots previously shown in Fig. 7. The area of a function or a filter correlates to the power of a filtered image. Area of each plot is normalised at the magnitude of the area for dark viewing condition. As can be seen, about 7 and 15 % of the loss in power was occurred under overcast and bright, respectively due to the increase of surround luminance. The amount of power loss caused by the reduction in contrast sensitivity can be analogous to that of Michelson contrast reduction. As given in Table 1, Michelson contrast decrease reaches up to approximately 10 and 18 % respectively for overcast and bright. It yields to the fact that the amount of physical contrast reduction is larger than that of power loss in CSF. In order
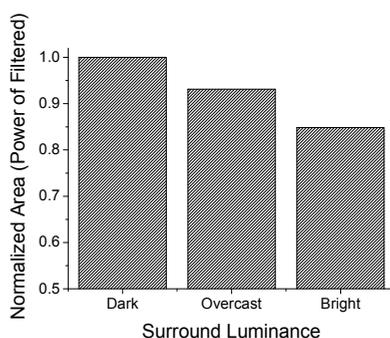
Fig. 8. Ratio of area of *psi* functions given in Figs. 4 (a) through (c). The area of a function or a filter correlates to the power of a filtered image. As can be seen, about 15 and 23% of the loss in power was occurred under overcast and bright, respectively due to the increase of ambient illumination.

to statistically verify the surround luminance and spatial frequency effects on the shape in CSF, two-way analysis of variance (ANOVA) was performed with surround luminance and spatial frequency as independent variables and contrast sensitivity as the dependent variable. Significant effects could be found for both surround luminance and spatial frequency. Their P values were less than 0.0001. A value of $P < 0.05$ was considered to be statistically significant in this study.

Generally, effect of surround luminance on the luminance CSF appears the same to that of mean luminance as previously discussed in Fig. 1. Because CSF response correlates to the filtered light in the ocular media, smaller CSF responses across the spatial frequency domain result in less power of the filtered image; thus, less amount of light can be perceived by the visual system. Therefore, the stimulus should appear darker under a higher surround luminance which can be verified through another set of experiments. The subsequent section discusses the results from Experiment 2.

**2.3.5 Change in brightness caused by surround luminance**

The mean perceived brightness magnitudes of the nine neutral colours for the 5 observers are drawn in Fig. 9. The abscissa shows measured luminance of the neutral patches shown on an LCD. The ordinate represents their corresponding perceived brightness magnitudes. The filled circles indicate dark, empty circles for overcast and crosses for bright. Data points are linearly interpolated. As can be seen, the all data points for overcast and bright are underneath data points for dark which means that their perceived brightness is decreased in general, as the ambient illumination and surround luminance increase in spite of the additional luminance increase by viewing flare. Similar results of brightness reduction between the surround and focal area can also be found in other works. (Wallach, 1948; Heinemann, 1955) Since brightness estimates are known for their subject variability, the individual data are also illustrated along with their mean for each viewing condition in Fig. 10. Filled circles show mean of the 5 observers and error bars show 95% confidential interval. As the all observations were accepted by the three observer variability tests in Table 2, the all brightness estimates follow the same trends. No particular outliers can be observed.
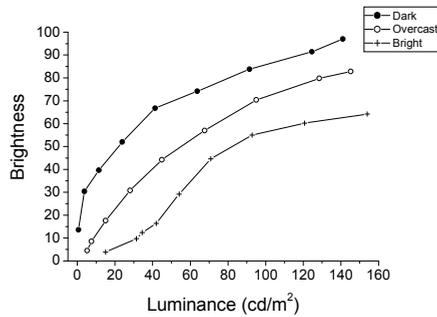
Fig. 9. Luminance vs. brightness under varied ambient illumination levels. The all data points for overcast and bright are underneath data points for dark which means that their perceived brightness is decreased in general, as the ambient illumination and surround luminance increase in spite of the additional luminance increase by viewing flare.



(a) Dark                                                            (b) Overcast
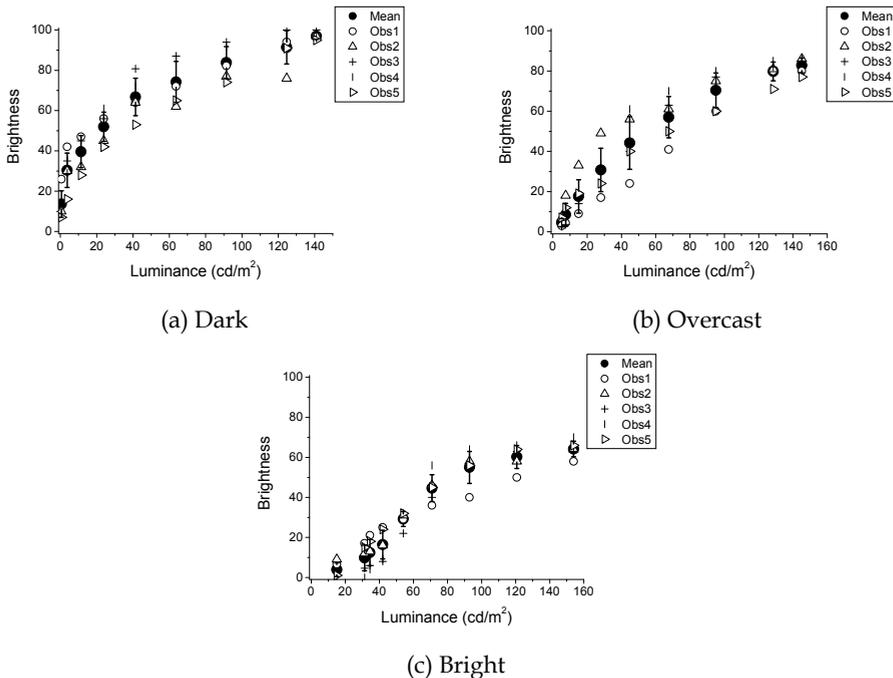


(c) Bright

Fig. 10. Individual brightness estimates for (a) dark (b) overcast and (c) bright. Brightness estimates are known for their subject variability but the all brightness estimates follow the same trends. No particular outliers can be observed. Error bars show standard error.

The precise relation between perceived brightness and stimulus luminance has been extensively studied using reflective colour samples. Traditionally, there are two most

frequently cited explanations. (Jameson & Hurvich, 1961) One of them is called *law of retinal stimulus*. It is intuitively expected that, if the amount of light falling on a given stimulus is increased, the intensity of the retinal light image could be increased and the HVS could perceive its increased brightness. All of the stimuli should appear lighter with the aid of increased luminance from ambient illumination. The other most frequently cited explanation for the relation between perceived brightness and stimulus luminance is *law of brightness constancy* (Wallach, 1948; Woodworth & Schlosberg, 1954; Jameson & Hurvich, 1959, 1961). This phenomenon is based on neural processing after light rays pass through ocular media in the HVS. There are some examples that apparent brightness of visually perceived objects is relatively constant in real world: white snow always appears bright but black coal looks very dark regardless a range of illuminance. Specifically, although the coal in the high illumination may actually reflect more intensity of light to the eye than does the snow at the low illumination. According to this theory, the relative brightness between with and without ambient illumination should be constant. However, our experimental results showed reduction in perceived brightness under ambient illumination and neither of the two traditional phenomena could predict this situation. One of the possible reasons for this is that the lighter surround makes the focal area appears darker and this phenomenon is referred to as simultaneous lightness contrast. (Palmer, 1999) The neural contrast mechanism that makes the low-luminance areas appear darker in bright environments more than compensates for the reduced physical contrast caused by intraocular scatter. (Stiehl et al., 1983; Wetheimer & Liang, 1995)

## 2.4 Summary

This section examined the variation in shape of spatial luminance CSF under different surround luminance levels and reduction in brightness of uniform neutral patches shown on a computer controlled display screen is also assessed to explain change of CSF shape. In specific, Experiment 1 was conducted to measure the compound results of contrast threshold perception and physical contrast decrease of a display resulted from the increase of ambient illumination. The former is found to be attributed by simultaneous lightness contrast (Palmer, 1999) between stimuli on a display and surround luminance so yields to cause the change in CSF shape. The latter is usually decreased by the surface light reflections off the front of the monitor screen referred to as viewing flare. Through a set of brightness magnitude estimations in Experiment 2 the surround luminance effects on the CSF and brightness reduction assumption could be justified. The viewing flare and display terms were successfully deducted by using MTF. Consequently, a large amount of reduction in contrast sensitivity at middle frequency area ($4 < u < 13$) can be observed; however, little reduction in contrast sensitivity is found for lower frequencies ($u < 4$). They show band-pass characteristics and the spatial frequency where the maximum contrast sensitivity occurs moves from 5 to 4 cpd when surround luminance increases from dark to overcast to bright. However, it is not quite easy to yield significance of the shift on the sampling frequency of 1 cpd. Generally, effect of surround luminance on the luminance CSF appears the same to that of mean luminance. Because CSF response can correlate to the filtered light in the ocular media, smaller CSF responses across the spatial frequency domain result in less power of the filtered image; thus, less amount of light can be perceived by the visual system. Therefore, the stimulus should appear dimmer under a higher surround luminance. The power loss in CSF reaches up to 7 and 15 % respectively for overcast and bright. Analogously, the Michelson contrast decrease was 10 and 18 % for overcast and bright. It yields to the fact that the amount of physical contrast reduction

is larger than that of power loss in CSF. The statistical significance of the surround luminance and spatial frequency effects on the shape in CSF, two-way ANOVA was performed and significant effects could be found for both parameters.

The results, which can be obtained from Experiments 1 and 2, are applicable to various purposes. Since CSFs have been widely used for evaluating image quality by predicting the perceptible differences between a pair of images (Barten, 1990; Daly, 1993; Zhang & Wandell, 1996; Wang & Bovik, 1996) surround luminance effects on CSF can be very useful for this application. Furthermore, the results can also be applied to simulate the appearance of a scene (Peli, 1996, 2001) and evaluate the visual performance of the eye. (Yoon & Williams, 2002)

## 3. Evaluating image quality

This section intends to quantify the effects of the surround luminance and noise of a given stimulus on the shape of spatial luminance CSF and to propose an adaptive image quality evaluation method. The proposed method extends a model called square-root integral (SQRI). The non-linear behaviour of the human visual system was taken into account by using CSF. This model can be defined as the square root integration of multiplication between display modulation transfer function and CSF. The CSF term in the original SQRI was replaced by the surround adaptive CSF quantified in this study and it is divided by the Fourier transform of a given stimulus for compensating for the noise adaptation.

### 3.1 Backgrounds
### 3.1.1 Adaptation to spatial frequency of the stimulus
On spatial frequency adaptation, (Fairchild & Johnson, 2007) proposed adjusting two-dimensional CSF based on the degree of a given image's blurness. (Goldstein, 2007) demonstrates spatial frequency adaptation effect as shown in Fig. 11. The left pair consists of patterns having different spatial frequency. Spatial frequency of the upper pattern shows lower than that of the lower pattern. However, the other pair on the right-handed side has two patterns showing the identical spatial frequency. After staring at the bar on the left pair of patterns for a while, the other pair on the right handed side appear to shift in spatial frequency in directions opposite the adapting stimuli (the left pair).

More precisely, a half of the foveal area of the viewer is adapted to the lower frequency of the upper pattern, while the other half of the foveal area is adapted to the higher frequency of the lower pattern. After adapting to the spatial frequency of those stimuli, although the two identical patterns were assessed, the upper right and lower right patterns should appear to show higher and lower spatial frequencies, respectively. Consequently, the adapted contrast sensitivity of the HVS can be related to the reciprocal of the adapting stimulus' spatial frequency as given by (Fairchild & Johnson, 2007)

$$CSF_a(u) = \frac{CSF(u)}{img(u)+1} \tag{11}$$

where $img(u)$ is Fourier transform of a given image.

### 3.1.2 Square-root integral
The SQRI method (Barten, 2006) can be defined as the square root integration of multiplication between display MTF, i.e., $MTF(u)$ and CSF, the reciprocal of contrast threshold function $M_t(u)$ as

$$SQRI = \frac{1}{\ln 2} \int_0^{u_{\max}} \sqrt{\frac{MTF(u)}{M_t(u)}} \frac{du}{u} \tag{12}$$

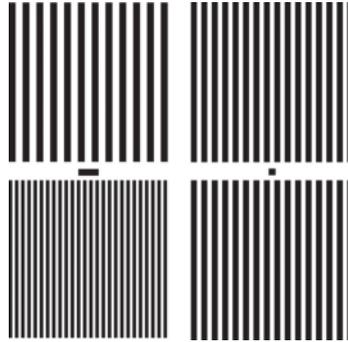where $u_{max}$ is the maximum spatial frequency to be displayed.



Fig. 11. Demonstration of spatial frequency adaptation

## 3.2 Modelling the effects of surround luminance

The surround luminance effects on CSF are quantified in this section. In order to compensate for the effects, a weighting function $\varphi$ was multiplied to the adapting luminance that is denoted as $L$ in (Barten, 1990). Precisely, as previously mentioned in Background section, brightness of a stimulus can be affected by surround luminance increase so a function $\varphi$ should be multiplied to $L$. For each surround, the following optimisation process was carried out.

Step 1. A CSF curve is predicted using Barten's model under a given surround condition. The adapting luminance can be obtained by measuring the mean luminance between black and white patches of the display.

Step 2. The predicted CSF curve is adjusted by changing the value of $\varphi$ so that its maximum contrast sensitivity value can match that of the measured CSF data in (Kim & Kim, 2010) under the given surround condition. Note: in case the surround is dark, $\varphi$ should equal to one.

Consequently, the maximum contrast sensitivity value of the adjusted CSF curve for overcast could match that of the measured CSF data points when $\varphi$ equals to 0.534. In the case of bright, $\varphi$ is found to be 0.339. Table 3 lists the obtained optimum $\varphi$ values for the three surrounds along with their measured surround luminance levels. The relation between $\varphi$ against the corresponding surround luminance ($L_S$) can be modelled by an exponential decay fit as given in eq. (13) and also illustrated in Fig. 12. Its exponential decaying shape appears similar to that of the image colour-quality model (Kim et al., 2007) that predicts the overall colour-quality of an image under various outdoor surround conditions. In addition, the change in "clearness," which is one of the psychophysical image quality attributes, caused by the illumination increase could also be modelled by an exponential decay function as well. (Kim et al., 2008)

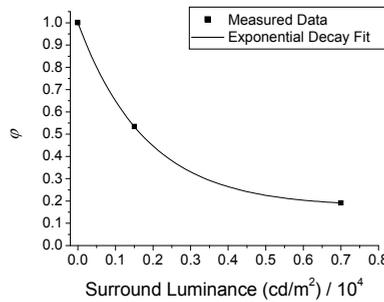$$\varphi = 0.17 + 0.83 e^{-10^{-4} \cdot L_S / 0.18} \tag{13}$$

Fig. 12. Relation between the surround luminance factor ($\varphi$) and the normalised surround luminance ($L_S$ /$10^4$)

### 3.3 Proposed method: Adaptive SQRI

The proposed method - adaptive SQRI ($SQRI_a$) - can be expressed as eq. (14). The $M_t(u)$ in the original SQRI (see eq. (12)) is replaced by $M_{ta}(u)$ which represents the inverse of the adaptive CSF denoted as $CSF_a(u)$.

$$SQRI_a = \frac{1}{\ln 2}\int_0^{u_{max}} \sqrt{\frac{MTF(u)}{M_{ta}(u)}}\,\frac{du}{u} \tag{14}$$

where $u$ denotes the spatial frequency and $1/M_{ta}(u)$ is

$$\frac{1}{M_{ta}(u)} = CSF_a(u) = \frac{au\exp(-bu)\sqrt{(1+c\exp(bu))}}{(k\times img(u)+1)}$$

The numerator of $CSF_a$ shows the surround luminance adaptive CSF; $a$, $b$, and $c$ are

$$a = \frac{540\left(1+0.7/\varphi L\right)^{-0.2}}{1+\dfrac{12}{w\left(2+u/3\right)^2}}$$

$$b = 0.3\left(1+100/\varphi L\right)^{0.15}$$

$$c = 0.06$$

where the adapting luminance $L$ is the mean luminance between white and black on the display under a given surround luminance and $\varphi$ is a weighting function for the surround luminance effect as previously given in eq. (13).

As (Fairchild & Johnson, 2007) found the reciprocal relation between the adapted contrast sensitivity of the HVS and the adapting stimulus' spatial frequency, as shown in eq. (11), $CSF_a$ is divided by Fourier transform of the given image. The denominator of the $CSF_a$ shows amplitude of the Fourier transformed image information, $img(u)$. A constant $k$ is multiplied to the magnitude of $img($u$)$ for normalisation as

$$k = 10^4 \times \frac{1}{\max(|img(u)|)} \qquad (15)$$

Since the denominator of $SQRI_a$ is Fourier transform of a given image, the model prediction can be proportional to the inverse of the image's spatial frequency. In order to attenuate any unwanted spatial frequency dependency of the image, the model prediction should be normalised by that of a certain degraded image expressed as

$$nSQRI_a = \frac{SQRI_a(Original)}{SQRI_a(Degraded)} \qquad (16)$$

where $nSQRI_a$ denotes a normalised $SQRI_a$ prediction and $SQRI_a$ (*Original*) and $SQRI_a$ (*Degraded*) respectively represent $SQRI_a$ predictions for a given original image and its degraded version.

The degraded image can be defined as an image of which its pixel resolution is manipulated to a considerably lower level, i.e., 80 pixels per inc. (ppi), while the original resolution was 200 ppi., and luminance of each pixel is reduced to 25 % of its original. The normalisation method makes $SQRI_a$ to predict the quality score of a given image regardless the level of adapting spatial frequency. Since the overall dynamic range of $nSQRI_a$ in eq. (16) may be changed due to the normalisation process, it was re-scaled to a 9-category subjective scale (Sun & Fairchild, 2004) using a least-square method for each surround luminance condition. The rescaling process can be written as

$$J' = pJ + q \qquad (17)$$

where $J'$ represents a re-scaled 9-category value of $J$, i.e., $nSQRI_a$ of an image. The scaling factors are denoted as $p$ (slope) and $q$ (offset) and the optimum scaling factors can be determined through the subsequently discussed psychophysical test.

### 3.4 Subjective experimental setup

In total, five test images were selected for image quality evaluation in this study. They contained sky, grass, water, facial skin (Caucasian, Black, and Oriental) and fruit scenes, as shown in Fig 13. Those images were displayed on a 22.2-inc. Eizo ColorEdge221 LCD. The maximum luminance producible is approximately 140 cd/m$^2$ in a dark room and the black level elevates up to 1 cd/m$^2$ due to the inherent leakage light problem of typical LCDs. The display was illuminated by using an EVL Lighting Colourchanger 250 light source in a diagonal direction. More details about the experimental setting are described in the previous section. The surround luminance and the viewing conditions are summarised in Table 1.

Each image was manipulated in terms of the three attributes, blurrness, brightness and noisiness. For adjusting those attributes, resolution, luminance and noise level of the images were controlled. Specifically, the five images were manipulated by changing their resolution from 200 (original) to 80 ppi with steps of 40 ppi (original + 3 resolution degradations), luminance from 100 (original) to 25% with steps of 25% (original + 3 luminance reductions) and adding the Gaussian noise by changing the variance of the Gaussian function from 0 (original) to 0.006 with steps of 0.002 (original + 3 noise additions).

In total, for each test image, 64 images (4 resolution × 4 luminance × 4 noise) were produced by the image rendition when simultaneous variations are included. However, the

(a)                    (b)                    (c)                    (d)                    (e)
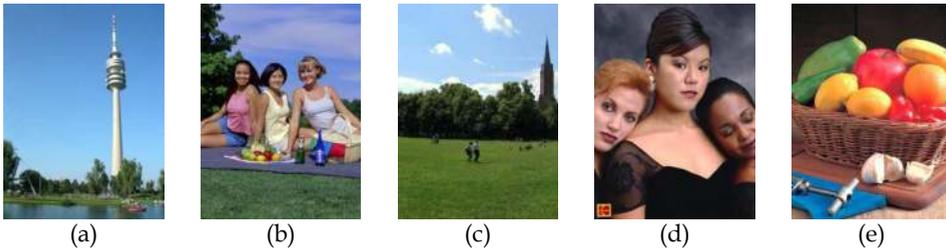
Fig. 13. Test images (a) Skytower, (b) Picnic, (c) Grass, (d) Ladies, and (e) Fruits

combinations between lower levels of the rendition-parameters resulted in considerably low quality images, which can be rarely seen in real world so were excluded. Figure 14 shows the sampled 22 images out of 64 in an image rendering cube. Each axis represents each of the three rendered parameters: resolution, luminance and noise. The coordinates (0, 0, 0) is the original image and larger numbers represent lower levels of each parameter.
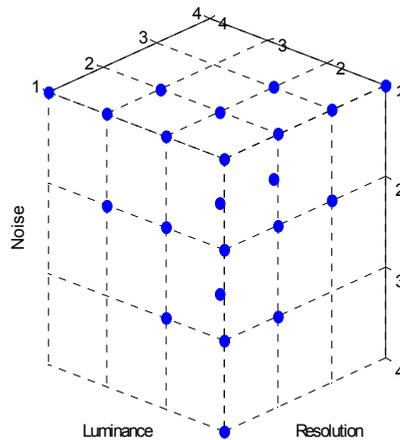


Fig. 14. Sampled images

Among 110 images for 5 distinct test images, only 35 images were randomly selected and used. Those selected images are listed in Table 4, where FR is for 'Fruits', GR for 'Grass', LD for 'Ladies', PC for 'Picnic', SK for 'Skytower'. The four rendition levels for each of the three image parameters (Resolution; R, Luminance; L and Noise; N) are indicated as numbers from 0 to 3, where 0 is the original. The images were processed by the proposed algorithm for the three different surround levels: dark, overcast and bright. A panel of 9 observers with normal colour vision (5 females and 4 males; 26~38 years old) were asked to judge the quality of the rendered images on the mobile LCD from the distance of 25 centimetres (accommodation limit), using a 9-point scale (1 to 9). This subjective image quality judgment procedure was repeated under the three different surround conditions. Therefore, the total number of psychophysical assessments can be 845 (35 images × 9 observers × 3 viewing conditions). The collected subjective data were averaged for each image. This is a ITU-R BT.500-11 method for analysing the category judgment data. (ITU-R, 2002)

| FR | | | | GR | | | | LD | | | | PC | | | | SK | | | |
|---|---|---|---|---|---|---|---|---|---|---|---|---|---|---|---|---|---|---|---|
| | R | L | N | | R | L | N | | R | L | N | | R | L | N | | R | L | N |
| FR1 | 0 | 0 | 3 | GR1 | 0 | 0 | 2 | LD1 | 0 | 1 | 0 | PC1 | 0 | 0 | 0 | SK1 | 0 | 0 | 0 |
| FR2 | 0 | 1 | 0 | GR2 | 0 | 0 | 3 | LD2 | 0 | 1 | 1 | PC2 | 0 | 1 | 1 | SK2 | 0 | 0 | 2 |
| FR3 | 0 | 1 | 2 | GR3 | 0 | 1 | 1 | LD3 | 0 | 2 | 1 | PC3 | 0 | 2 | 1 | SK3 | 0 | 0 | 3 |
| FR4 | 0 | 2 | 0 | GR4 | 0 | 3 | 0 | LD4 | 1 | 0 | 1 | PC4 | 1 | 0 | 2 | SK4 | 0 | 3 | 0 |
| FR5 | 0 | 3 | 0 | GR5 | 1 | 1 | 0 | LD5 | 1 | 1 | 1 | PC5 | 1 | 2 | 0 | SK5 | 1 | 1 | 0 |
| FR6 | 1 | 0 | 2 | GR6 | 1 | 2 | 0 | LD6 | 2 | 0 | 0 | PC6 | 3 | 0 | 0 | SK6 | 2 | 0 | 0 |
| FR7 | 1 | 2 | 0 | GR7 | 3 | 0 | 0 | | | | | | | | | SK7 | 2 | 1 | 0 |
| FR8 | 2 | 1 | 0 | | | | | | | | | | | | | SK8 | 2 | 1 | 1 |

Table 4. The Randomly Selected Test Images

## 3.5 Results
### 3.5.1 Observer variation
The mean CV of the all observers participated in this experiment ranged from 20 to 39, and the grand mean CV across the observers and the 5 test stimuli for dark surround condition was 26, which is thought of as acceptable. (Note that CV value of 26 means 26% error of individual from the arithmetic mean.) The mean observer accuracy was found to be 32 for overcast and 30 for bright which are also within the acceptable CV boundary. The results also indicate that there was not much variation in terms of CV values between different experimental phases and image contents. One of the observers showed a relatively higher CV (39) than the other observations, but its impact to the grand mean (29) was not large thus was included for further analysis and modelling procedures.

### 3.5.2 Prediction accuracy of the proposed algorithm
Figure 15 presents box plots for comparing subjective image quality scores between the 3 surround conditions including dark, overcast and bright. Box is drawn between the lower and upper quartiles and a line across each box represents the median. Whiskers are extended to smallest and largest observations or 1.5 times length of box. In general, the range of subjective data could be decreased as the surround luminance increases. For example, MOS is 5.4 under dark, 4.7 under overcast and 3.5 under bright. It can be seen from the box plots that MOS difference between the viewing conditions is significant.
Scaling factors in eq. (13) optimised for the three viewing conditions are listed in Table 5. Magnitude of them is systematically changed from dark to overcast to bright and could be modelled by an exponential decay fit of surround luminance (see eqs. (18) and (19)). The predicted curves are compared with the computed scaling factors as illustrated in Fig 16.

$$p = 1.16 + 2.36e^{-10^{-4}L_S/0.35} \tag{18}$$

$$q = 0.35 - 5.38e^{-10^{-4}L_S/0.29} \tag{19}$$

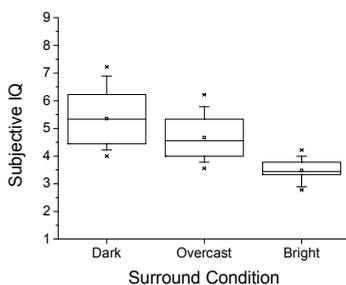where $L_S$ is the surround luminance level.

Fig. 15. Box plots for comparing subjective image quality scores between the 3 surround conditions including dark, overcast and bright. Box is drawn between the lower and upper quartiles and a line across each box represents the median. Whiskers are extended to smallest and largest observations or 1.5 times length of box. In general, the range of subjective data could be decreased as the surround luminance increases.

|        | Dark  | Overcast | Bright |
|--------|-------|----------|--------|
| Slope  | 3.93  | 2.69     | 1.47   |
| Offset | -6.71 | -2.89    | -0.11  |

Table 5. Scaling factors (slope and offset) for the three viewing conditions



|     (a)     |     (b)     |
|-------------|-------------|
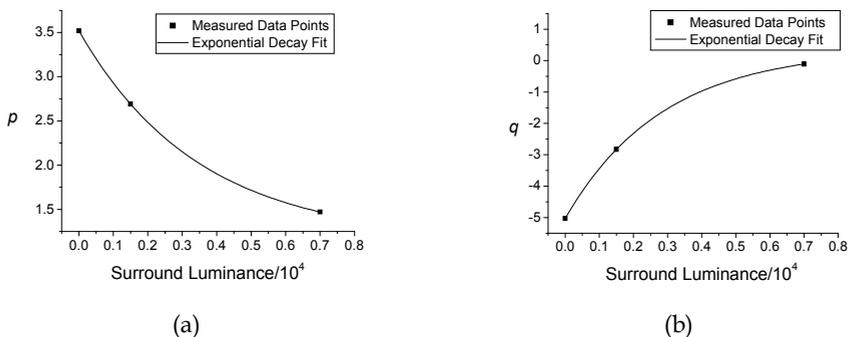
Fig. 16. Scaling factors as a function of surround luminance (a) Slope $p$ (b) Offset $q$

In Fig 17, the abscissa shows $nSQRI_a$ prediction values, which are re-scaled by the scaling factors listed in Table 5, and the ordinate shows the corresponding MOS. (Note that a 45° line is given for illustrating the data spread.) Different shaped symbols represent different test images. For instance, the filled squares are for "Fruits (FR)", circles for "Grass (GR)", triangles for "Ladies (LD)", crosses for "Picnic (PC)" and diamonds for "Skytower (SK)". The model accuracy for the overall data sets can also be predicted by calculating a CV value between the two axes and it was 15 which is smaller than the mean observer accuracy (29) across the three surround conditions. Specifically, the CV between the two data sets was 18 for dark, 13 for overcast and 9 for bright and all are less than the corresponding mean
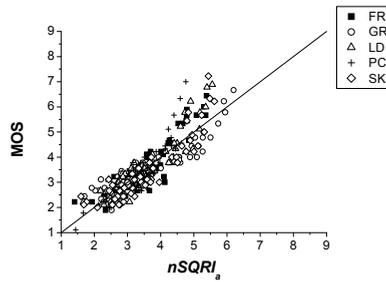
Fig. 17. Comparison between *nSQRIa* and their corresponding MOS across the three surround conditions

observer accuracy. Note that the mean observer accuracy was 26 for dark, 32 for overcast and 30 for bright. Consequently, no significant image dependency of the model prediction was observed due to the spatial frequency normalisation procedure.

### 3.6 Summary

The current research intends to quantify the surround luminance effects on the shape of spatial luminance CSF and to propose an image quality evaluation method that is adaptive to both surround luminance and spatial frequency of a given stimulus. The proposed image quality method extends to a model called SQRI. (Barten, 1990) The non-linear behaviour of the HVS was taken into account by using CSF. This model can be defined as the square root integration of multiplication between display MTF and CSF. It is assumed that image quality can be determined by considering the MTF of the imaging system and the CSF of human observers. The CSF term in the original SQRI model was replaced by the surround adaptive CSF quantified in this study and it is divided by the Fourier transform of a given stimulus. The former relies upon the surround factor function ($\varphi$) shown in eq. (13) and the latter requires a normalization procedure. The model prediction for a certain image is divided by that of its degraded image of which its pixel resolution is manipulated to be 80 ppi and luminance of each pixel is reduced to be 25% of its original. The model accuracy and observer accuracy are comparable in terms of CV. The mean model accuracy is a CV value of 15 and observer accuracy is 29. Consequently, the model accuracy outperformed the observer accuracy and no significant image dependency could be observed for the model performance.

A few limitations of the current work should be addressed and revised in the future study. First, the model parameters should be revised for larger sized images. A 2-inch mobile LCD is used to display images in this study so any image size effect on the model prediction should be verified in the future work. Second, more accurate model predictions may be achievable when the actual display MTF is measured and used instead of the approximation shown in eq. (9). Last but not least, a further improvement to the model prediction accuracy can be made when chromatic contrast loss of the HVS is taken into account.

## 4. Enhancing image quality

The loss in contrast discrimination ability of the human visual system was estimated under a variety of ambient illumination levels first. Then it was modelled as a non-linear

weighting function defined in spatial frequency domain to determine which of parts of the image, whatever their spatial frequency, will appear under a given surround luminance level. The weighting function was adopted as a filter for developing an image enhancement algorithm adaptive to surround luminance. The algorithm aims to improve the image contrast under various surround levels especially for small-sized mobile phone displays through gain control of a 2D contrast sensitivity function.

### 4.1 Proposed surround luminance adaptive image enhancement
### 4.1.1 Contrast sensitivity reduction of the HVS

As shown in the earlier section, Fig. 12 illustrates the relation between surround luminance level (cd/m²) and the surround effect function ($\varphi$). The shape of the function is similar to that of the image colour-quality decay function (Kim et al., 2007) that predicts the overall colour-quality of an image based upon measurable image-properties under various outdoor surround conditions. In addition, the change in 'clearness' caused by the illumination increase could also be modelled as an exponential decay function as well. (Kim et al., 2008)

CSFs for the three surrounds in total – dark (0 lx), overcast (6100 lx) and bright (32000 lx) – are computed using eqs. 13 and 14 and also plotted in Fig. 18 while other variables such as viewing distance and adapting luminance of a stimulus remain the same. The spatial frequency where the maximum contrast sensitivity occurred was moved toward a lower frequency from dark (4.4 cpd) to bright (3.8 cpd). As a result, the surround luminance increase resulted in approximately 7 and 15% loss in contrast sensitivity of the human visual system for overcast and bright, respectively. (Kim & Kim, 2010)
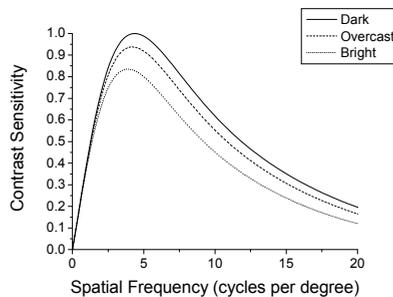


Fig. 18. Comparison of CSFs under dark and ambient illuminations

In order to compensate for the loss in image contrast caused by surround luminance increase and enhance the image quality, an adaptive enhancement gain control algorithm to the surround luminance was developed using an adaptive weighting filter. This filter correlates to the normalised contrast sensitivity difference between the reference (dark) and a target surround luminance level. The contrast sensitivity difference, $D(u,v)$, between the *reference* (dark), $CSF_R(u,v)$, and a given *target* surround, $CSF_T(u,v)$, represents the loss in image contrast caused by increase of the surround luminance which can be expressed as

$$D(u,v) = \left( CSF_R(u,v) - CSF_T(u,v) \right) \tag{20}$$

where $u$ and $v$ are frequency variables.

Since the image enhancement can be achieved, when an enhancement gain greater than 1 is multiplied to the amplitude of a given image, the offset of these weighting filters should be increased up to greater than 1 and a constant value of 1 was added to $D(u,v)$. In addition, the maximum value of $D(u,v)$ is also added to the offset so the adaptive weighting filter can be defined as

$$H(u,v) = D(u,v) + (1+C) \qquad (21)$$

where C = max($D(u,v)$).

The maximum value of $D(u,v)$ implies the change in brightness and the threshold level to be enhanced under a given surround luminance level. Since various spatial frequency levels are mixed in a complex image, the masking phenomenon (Wandell, 1995; Kim et al., 2007) can occur and there might be some contrast loss detectable in unexpected frequencies. The masking commonly occurs in multi-resolution representations and there are cases when two spatial patterns S and S + ΔS cannot be discriminated, while ΔS seen alone, can be visible. Therefore, all frequency regions should be enhanced globally by a certain level of enhancement gain threshold and such significant regions should be enhanced with higher weights. However, the enhancement threshold level was arbitrarily chosen as the maximum value of $D(u,v)$ in this study and more investigations are required in future study.

Figure 19 shows estimates of the adaptive weighting filter for the three surround levels: dark, overcast and bright, when a field size was 5 degrees and the display's adapting (mean) luminance was 89.17 cd/m². Since the loss in image contrast becomes larger, as the ambient illumination increases, the weighting filter response for bright surround shows the highest filter response and overcast surround follows. In case of dark surround, the amplitude of original image can be preserved as being multiplied by an enhancement gain of 1 across the all spatial frequencies. The enhancement threshold level is 0 for dark, 0.15 for overcast and 0.31 for bright. Since CSFs are known as smoothly varied band-pass filters, the enhancement gain can also be smoothly changed. The adaptive image enhancement filter can be defined as a weighting function to determine which of parts of the image, whatever their spatial frequency, should have a higher enhancement gain.
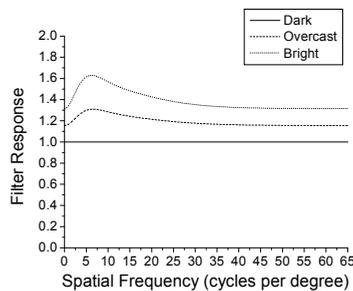
Fig. 19. The adaptive weighting filter estimates

## 4.2 Results

Figure 20 presents a test image and their enhanced images for the two surround conditions and their histograms of luminance of the composite channel (Luminosity). The input RGB

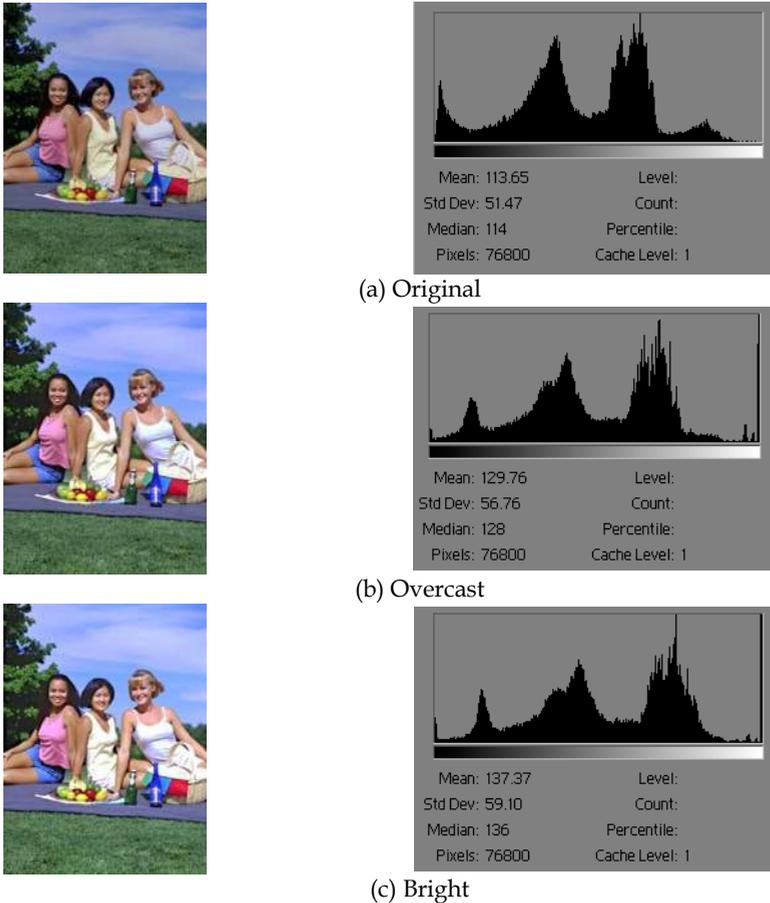(a) Original



(b) Overcast



(c) Bright

Fig. 20. Example of enhanced images and their luminosity histogram

values were converted into CIECAM02 (CIE, 2004) perceptual colour attributes such as *Jab* and *J* was then transformed into the recently updated *J'*. (Luo et al., 2006) Only lightness *J'* went into the enhancement procedure while chrominance properties *a* and *b* were preserved. The horizontal axis of each histogram represents the intensity values, or levels, from the darkest (0) at the far left to brightest (255) at the far right; the vertical axis represents the number of pixels with a given value. Moreover, the statistical information about the intensity values of the pixels appears below the histogram: mean, standard deviation (Std Dev), median, the number of pixels in the image and so forth.

As can be seen in Fig. 20, tonal variance in those histograms yields quite spread and both mean and standard deviation were increased as surround luminance increases. The mean was 113.65 for original, 129.76 for overcast and 137.37 for bright. The standard deviation was 51.47 for original, 56.76 for overcast and 59.10 for bright. Consequently, the overcall brightness and contrast of the image were increased. The resultant enhanced images may appear overexposed especially for the enhanced one for bright. However, if those images are seen with the surround luminance levels, they are supposed to show the similar degree of

image quality as the original seen under the reference (dark) viewing condition (as if reduced appetite leads to stronger taste of food).

Figures 21 (a) through (b) illustrate the comparison between enhanced and original images in terms of image quality scores judged by the nine observers. The abscissa represents subjective image quality score of the original images under a certain surround condition and the ordinate shows that of their enhanced images. For example, if most of the data points are upper the 45-degree line (red line), the enhanced images were judged as higher image quality. In general, majority of the data points were upper the 45-degree line for all of the surround conditions and it can be said that the enhanced images are rated by higher category values than their original images. When the proposed algorithm was applied for overcast condition data set, 74% (26 out of 35 images) subjective values of the enhanced images were higher than that of the original images (Fig. 21 (a)). In addition, its performance was more or less the same as the original images judged under dark viewing condition. In Fig. 7 (b), the images processed by the proposed algorithm for bright condition were compared with their corresponding original images. As well as overcast, the proposed algorithm produced better quality images than their original images seen under the same condition, 85% (30 out of 35 images). Subjective image quality score of the enhanced images was similar to that of original images judged under overcast surround condition. The 15% reduction caused in image quality could be due to the impairment in chromatic channels. Chromatic contrast should also be decreased under bright surrounds and the chromatic contrast loss effects will be left for the future work.
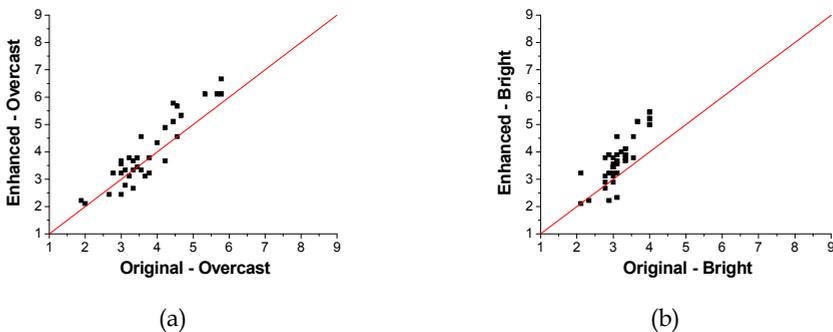


(a)                                          (b)

Fig. 21. Comparison between the original and enhanced image for each surround condition

One of possible artefacts that can be caused by the proposed algorithm is out boundary colours (OBC). Since a gain value larger than one is multiplied to a given image, some colours may lie outside colour gamut of the display. Those colours can be referred to as OBCs and more details can be found in Ref. 22. In this study, OBCs were clipped at the maximum value (255). However, the OBC effect may be overwhelmed by the contrast and brightness compensation so the artefact was not significantly perceptible during the psychophysical evaluations.

### 4.3 Summary

In this section, an adaptive image enhancement algorithm was proposed and their performance was observed through a set of subjective assessments. The contrast

discrimination ability of human observers under ambient illumination was quantified as a weighting function to determine which of parts of the image, whatever their spatial frequency, will appear under a certain surround luminance level. The weighting function was adopted as the image enhancement filter in spatial frequency domain. Most of the enhanced images were rated as higher image quality scores than their original images through a set of subjective validation experiment. The quality of images under bright surround was enhanced up to that of images seen under overcast. Similarly, the quality of images under overcast was reached that of image seen under dark. Further improvement of image contrast can be achieved when chromatic contrast loss is compensated that could be one of the afterthoughts.

## 5. Acknowledgment

## 6. References

Arend, L. E. and Spehar, B. (1993). Lightness, brightness and brightness contrast: I. Illumination variation. *Perception & Psychophysics*, Vol. 54, No. 4, (February 1933), pp. 446-456, ISSN 0031-5117

Arend, L. E. and Spehar, B. (1993). Lightness, brightness and brightness contrast: II. Reflectance variation. *Perception & Psychophysics*, Vol. 54, No. 4, (October 1993), pp. 457-468, ISSN 0031-5117

Barten , G. J. (1991). Resolution of liquid-crystal displays. *SID Digest*, ISSN 0003-966X

Barten, P. G. (1990). Evaluation of subjective image quality with the square-root integral method. *Journal of the Optical Society of America A*, Vol. 7, No. 10, (October 1990), pp. 2024-2031, ISSN 1084-2529

Barten, P. G. J. (1999). *Contrast Sensitivity of The Human Eye and Its Effects on Image Quality.* SPIE Press, ISBN 978-0819434968,Washington

Bartleson , J. (1984). *Optical Radiation Measurements*, Bartleson, C. J. & Grum, F. (Eds.), Academic Press, ISBN 978-0123049049, NY

Blakeslee, B., Reetz, D. and McCourt, M. E. (2008). Comping to terms with lightness and brightness: Effects of stimulus configuration and instructions on brightness and lightness judgments. *Journal of Vision*, Vol. 8, No. 11, (August 2008), pp. 1-14, ISSN 1534-7362

Braddick, O., Campbell, F. W. and Atkinson , J., (1978). Channels in vision: basic aspects, In : *Handbook of Sensory Physiology*, Held, R., Leibowitz H. W. and Teuber, H. –L. (Eds.), Springer-Verlag, ISBN 0-387-05146-5, New York

Burton, K. B., Owsley, C. and Sloane, M. E. (1993). Aging and neural spatial contrast sensitivity: photopic vision. *Vision Research*, Vol. 33, No. 7, (May 1993), pp. 939-946, ISSN 0042-6989

Campbell, F. W. and Green, D. G. (1965). Optical and retinal factors affecting visual resolution. *Journal of Physiology*, Vol. 181, No. 3 (December 1965), pp. 576-593, ISSN 0022-3751

Campbell, F.W. and Robson, J.G. (1968). Application of Fourier analysis to the visibility of gratings. *Journal of Physiology*, Vol. 197, No. 3, (August 1968), pp. 551-566, ISSN 0022-3751

Choi , S.Y., Luo, M.R. and Pointer, M.R., (2007). The Influence of the relative luminance of the surround on the perceived quality of an image on a large display, *Proceedings of 15th Color Imaging Conference*, ISBN 978-0-89208-294-0, Albuquerque, New Mexico, November 2007

CIE Publication 15.2, Colorimetry, 2nd Ed., Commission Internationale de l'Eclairage, Vienna, 1986.

CIE publication 159-2004, A colour appearance model for colour management systems: CIECAM02, Vienna, 2004.

Cox, M. J., Norma, J. H. and Norman, P. (1999). The effect of surround luminance on measurements of contrast sensitivity. *Ophthalmic and Physiological Optics*, Vol. 19, No. 5, (September 1999), pp. 401-414, ISSN 0275-5408

Dacey, D. M. and Lee, B. B. (1994). The blue-on opponent pathway in the primate retina originates from a distinct bistratified ganglion cell. *Nature*, Vol. 367, No. 6465, (February 1994), pp. 731-735, ISSN 0028-0836

Daly, S. (1993). The Visible Differences Predictor: An Algorithm for the Assessment of Image Fidelity, In: *Digital Images and Human Vision, Watson A. B.* (Ed.), MIT press, ISBN 978-0262231718, Cambridge, Massachusetts

DeValois, R.L., Morgan, H. and Snodderly, D.M. (1974). Psychophysical studies of monkey vision – III. Spatial luminance contrast sensitivity tests of macaque and human observers. *Vision Research*, Vol. 14, No. 1, (January 1974), pp. 75-81, ISSN 0042-6989

Enroth-Cugell, C. and Robson, J. G. (1966). The contrast sensitivity of retinal ganglion cells of the cat. *Journal of Physiology*, Vol. 187, No. 3, (December 1966), pp. 517-552, ISSN 0022-3751

Fairchild, M. D. and Johnson, G. M. (2007). Measurement and modelling of adaptation to noise in image. *Journal of the Society for Information Display*, Vol. 15, No. 9, (September 2007), pp. 639-647, ISSN 1071-0922

Fairchild, M. D. and Reniff, L. (1995). Time-course of chromatic adaptation for color-appearance judgements. *Journal of the Optical Society of America A* Vol. 12, No. 5, (May 1995), pp. 824–833, ISSN 1084-2529

Goldstein , E. B. (2007). *Sensation and Perception, Thomson Wadsworth*, ISBN 978-0-495-27479-7, CA

Graham, N. (1980) Spatial-frequency channels in human vision: detecting edges without edge-detectors, In: *Visual Coding and Adaptability*, Harris, C. S. (Ed.), Erlbaum, ISBN 978098590166, Hillsdale, New Jersey

Heinemann, E. G. (1955). Simultaneous brightness induction as a function of inducing and test-field luminances. *Journal of Experimental Psychology*, Vol. 50, No. 2, (August 1955), pp. 89-96, ISSN 0096-3445

Higgins, K. E., Jaffe, M. J., Caruso, R. C. and deMonasterio, F. (1988). Spatial contrast sensitivity: effects of age, test-retest, and psychophysical method. *Journal of the Optical Society of America A*, Vol. 5, No. 12, (December 1988), pp. 2173-2180, ISSN 1084-2529

ITU-R Rec. BT. 500-10, Methodology for the subjective assessment of the quality of television pictures, Geneva, 2002.

Jameson, D. and Hurvich, L. M. (1959). Perceived color and its dependence on focal, surrounding, and preceding stimulus variables. *Journal of the Optical Society of America*, Vol. 49, No. 9, (September 1959), pp. 890-898, ISSN 108-7529

Jameson, D. and Hurvich, L. M. (1961). Complexities of perceived brightness. *Science*, Vol. 133, No. 1, (January 1961), pp. 174-179, ISSN 1545-1003

Johnston, A. (1987). Spatial scaling of central and peripheral contrast-sensitivity functions. *Journal of the Optical Society of America A*, Vol. 4, No. 8, (August 1987), pp. 1583-1593, ISSN 1084-2529

Katoh, N., Nakabayashi, K., Ito, M., and Ohno, S. (1998). Effect of ambient light on the color appearance of softcopy images: Mixed chromatic adaptation for self-luminous displays. *Journal of Electronic Imaging*, Vol. 7, No. 4, (October 1998), pp. 794-806, ISSN 1017-9909

Kim, Y. J. and Kim, H. (2010). Spatial luminance contrast sensitivity: Effects of surround. *Journal of the Optical Society of Korea*, Vol. 14, No. 2, (April 2010), pp.152-162, ISSN 1226-4776

Kim, Y. J., Bang, Y. and Choh, H. (2010). Gradient approach to quantify the gradation smoothness for output media. *Journal of Electronic Imaging*, Vol. 19, No. 1, (January 2010), pp. 011012, ISSN 1017-9909

Kim, Y. J., Bang, Y. and Choh, H. (2010). Measurement and modelling of vividness perception and observer preference for color laser printer quality. *Journal of Imaging Science and Technology*, Vol. 54, No. 1, (January 2010), pp. 010501, ISSN 1062-3701

Kim, Y. J., Luo, M. R., Choe, W., Kim, H.S., Park, S.O., Baek, Y, Rhodes, P., Lee, S. and Kim, C. (2008). Factors Affecting the Psychophysical Image Quality Evaluation of Mobile Phone Display: the Case of Transmissive LCD. *Journal of the Optical Society of America A*, Vol. 25, No. 9, (September 2008), pp. 2215-2222, ISSN 1084-2529

Kim, Y. J., Luo, M. R., Rhodes, P, Westland, S., Choe, W., Lee, S., Lee, S., Kwak, Y., Park, D. and Kim, C. (2007). Image-Colour Quality Modelling under Various Surround Conditions for a 2-inch Mobile Transmissive LCD. *Journal of the Society for Information Display*, Vol. 15, No. 9, (September 2007), pp. 691-698, ISSN 1071-0922

Kitaguchi, S., MacDonald, L., and Westland, S. (2006). Evaluating contrast sensitivity, *Proceedings of SPIE, Human vision and electronic imaging XI*, ISBN 9780819460974, Westlandm, Stephen, February 2006

Koenderink, J. J., Bouman, M. A., Bueno de Mesquita, A. E. and Slappendale, S. (1979). Perimetry of contrast detection thresholds of moving spatial sine wave patterns, Parts I-IV. *Journal of the Optical Society of America*, Vol. 68, No. 6, (June 1978), pp. 845-865, ISSN 108-7529

Lee, H. J., Choi, D. W., Lee, E., Kim, S. Y., M, Shin., Yang, S. A., Lee, S. B., Lee, H. Y. and Berkeley, B. H. (2009). Image sticking methods for OLED TV applications, *Proceedings of International Meeting on Information Display*, ISBN 1738-7558, Ilsan, Korea, October 2009

Li, Z., Bhomik, A.K., and Bos, P.J. (2008). Introduction to Mobile Displays, In: *Mobile Displays Technology and Applications*, Wiley, ISBN 978-0470723746, Chichester , UK

Liu C. & Fairchild M.D. (2004). Measuring the relationship between perceived image contrast and surround illumination, *Proceedings of IS&T/SID 12th Color Imaging Conference*, ISBN 978-0-89208-294-0, Scottsdale, Arizona, November 2004

Liu, C. & Fairchild, M.D. (2007). Re-measuring and modeling perceived image contrast under different levels of surround illumination, *Proceedings of IS&T/SID 15th Color Imaging Conference*, ISBN 978-0-89208-294-0, Albuquerque, New Mexico, November 2007

Luo, M. R., Clarke, A. A., Rhodes, P., Schappo, A., Scrivener, S. A. R., and Tait, C. J. (1991). Quantifying Colour appearance. Part 1. Lutchi colour appearance data. *Color Research and Application*, Vol. 16, No. 3, pp. 166, ISSN 0361-2317

Luo, M.R., Cui, G. and Rigg, B. (2001). The development of the CIE 2000 colour-difference formula: CIEDE2000. *Color Research and Application*, Vol. 26, No. 5, (August 2001), pp. 340-350, ISSN 0361-2317

Martinez-Uriegas, E. (2006). Spatial and Temporal Problems of Colorimetry, In: *Colorimetry: Understanding the CIE System*, CIE, ISBN 978-0-470-04904-4, Switzerland

Martinez-Uriegas, E., Larimer J.O., Lubin J. and Gille, J. (1995). Evaluation of image compression artefacts with ViDEOS, a CAD system for LCD color display design and testing, Proceeding series

Mornoney, N., Fairchild, M. D., Hunt, R. W. G., Li, C., Luo, M. R. and Newman, T. (2002). The CIECAM02 color appearance model, *Proceedings of 10th Color Imaging Conference*, Scottsdale, Arizona, November 2002

Owsley, C., Sekuler, R. and Siemsen, D. (1983). Contrast sensitivity throughout adulthood. *Vision Research*, Vol. 23, No. 7, (July 1983), pp. 689-699, ISSN 0042-6989

Palmer, S. (1999). *Vision science: Photons to Phenomenology*, MIT Press, ISBN 978-0262161831, Cambridge, Massachusetts

Pardhan, S. (2004). Contrast sensitivity loss with aging: sampling efficiency and equivalent noise at different spatial frequencies. *Journal of the Optical Society of America A*, Vol. 21, No. 2, (February 2004), pp. 169-175, ISSN 1084-2529

Park, Y., Li, C., Luo, M.R., Kwak, Y., Park, D. and Kim, C. (2007). Applying CIECAM02 for mobile display viewing conditions, *Proceedings of 15th Color Imaging Conference*, ISBN, Albuquerque, New Mexico, November 2007

Patel, A.S. (1966). Spatial resolution by the human visual system. *Journal of the Optical Society of America*, Vol. 56, No. 5, (May 1966), pp. 689-694, ISSN 108-7529

Peli, E. (1996). Test of a model of foveal vision by using simulations. *Journal of the Optical Society of America A*, Vol. 13, No. 6, (June 1996), pp. 1131-1138, ISSN 1084-2529

Peli, E. (2001). Contrast sensitivity function and image discrimination. *Journal of the Optical Society of America A*, Vol. 18, No. 2, (February 2001), pp. 283-293, ISSN 1084-2529

Post, D.L. and Calhoun, C.S. (1989). An evaluation of methods for producing desired colors on CRT monitors. *Color Research and Application*, Vol. 14, No. 4, (month and year of the edition), pp. 172-186, ISSN 0361-2317

Rohaly, A. M. and Buchsbaum, G. Global (1989). Spatiochromatic mechanism accounting for luminance variations in contrast sensitivity functions. *Journal of the Optical Society of America A*, Vol. 6, No. 2, (February 1989), pp. 312-317, ISSN 1084-2529

Rohaly, A. M. and Owsley, C. (1993). Modeling the contrast-sensitivity functions of older adults. *Journal of the Optical Society of America A*, Vol. 10, No. 7, (July 1993), pp. 1591-1599, ISSN 1084-2529

Rovamo, J., Virsu, V. and Nasanen, R. (1978). Cortical magnification factor predicts the photopic contrast sensitivity of peripheral vision. *Nature*, Vol. 271, No. 5640, (January 1978), pp. 54-56, ISSN 0028-0836

Rudd, M. E. and Popa, D. (2007). Stevens's brightness law, contrast gain control, and edge integration in achromatic color perception: a unified model. *Journal of the Optical Society of America A*, Vol. 24, No. 9, (September 2007), pp. 2766-2782, ISSN 1084-2529

Schade, O. H. (1956). Optical and photoelectric analog of the eye. *Journal of the Optical Society of America*, Vol. 46, No. 9a, (September 1956), pp. 721-739, ISSN 108-7529

Snodderly, D. M., Weinhaus, R. S. and Choi, J. C. (1992). Neural-vascular relationships in central retina of macaque monkeys (Macaca fascicularis). *Journal of Neuroscience*, Vol. 12, No. 4, (April 1992), pp. 1169-1193, ISSN 1529-2401

Stiehl, W. A., McCann, J. J. and Savoy, R. L. (1983). Influence of intraocular scattered light on lightness-scaling experiments. *Journal of the Optical Society of America*, Vol. 73, No. 9, (September 1983), pp. 1143-1148, ISSN 108-7529

Sun, Q. and Fairchild, M. D. (2004). Image Quality Analysis for Visible Spectral Imaging Systems. *Journal of Imaging Science and Technology*, Vol. 48, No. issue number, (month and year of the edition), pp. 211-221, ISSN 1062-3701

Tulunay-Keesey, U., Ver Hoever, J. N. and Terkla-McGrane, C. (1988). Threshold and suprathreshold spatiotemporal response throughout adulthood. *Journal of the Optical Society of America A*, Vol. 5, No. 12, (December 1988), pp. 2191-2200, ISSN 1084-2529

Van Nes, F. L. and Bouman, M. A. (1967). Spatial modulation transfer in the human eye. *Journal of the Optical Society of America*, Vol. 57, No. 3, (March 1967), pp. 401-406, ISSN 108-7529

Wallach, H. (1948). Brightness constancy and the nature of achromatic colors. *Journal of Experimental Psychology*, Vol. 38, No. 3, (June 1948), pp. 310-324, ISSN 0096-3445

Wandell, B.A. (1995). *Foundations of Vision*, Sinauer Associates, ISBN 0878938532, Sunderland, Massachusetts

Wang, Z. & Bovik , A. C. (2006). *Modern image quality assessment*, Morgan & Claypool Publishers, ISBN 978-1598290226, New Jersey

Watson, A.B. (2000). Visual detection of spatial contrast patterns: Evaluation of five simple models. *Optics Express*, Vol. 6, No. 1, (January 2000), pp. 12-33, ISSN 1094-4087

Westheimer, G. and Liang, J. (1995). Influence of ocular light scatter on the eye's optical performance. *Journal of the Optical Society of America A*, Vol. 12, No. 7, (July 1995), pp. 1417-1424, ISSN 1084-2529

Westland, S., Owens, H., Cheung, V. and Paterson-Stephens, I. (2006). Model of luminance contrast-sensitivity function for application to image assessment. *Color Research and Application*, Vol. 31, No. 4, (June 2006), pp. 315-319, ISSN 0361-2317

Woodworth, R. S. & Schlosberg, H. (1954). *Experimental psychology*, Holt, ISBN 101-179-848, New York

Wright, M. J. and Johnston, A. (1983). Spatiotemporal contrast sensitivity and visual field locus. *Vision Research*, Vol. 23, No. 10, (October 1983), pp. 983-989, ISSN 0042-6989

Yoon, G. and Williams, D. R. (2002). Visual performance after correcting the monochromatic and chromatic aberrations of the eye. *Journal of the Optical Society of America A*, Vol. 19, No. 2, (February 2002), pp. 266-275, ISSN 1084-2529

Zhang, X.M. & B. A,Wandell. (1996). A spatial Extension to CIELAB for digital color image reproduction, *Proceedings of the SID Symposiums*, ISSN 0003-966X
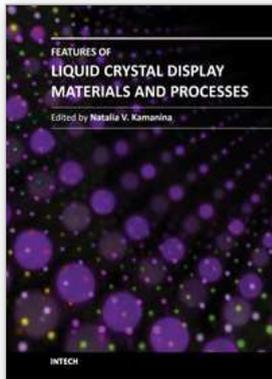
**Features of Liquid Crystal Display Materials and Processes**

Edited by Dr. Natalia Kamanina

Following the targeted word direction of Opto- and Nanoelectronics, the field of science and technology related to the development of new display technology and organic materials based on liquid crystals ones is meeting the task of replacing volume inorganic electro-optical matrices and devices. An important way in this direction is the study of promising photorefractive materials, conducting coatings, alignment layers, as well as electric schemes that allow the control of liquid crystal mesophase with good advantage. This book includes advanced and revised contributions and covers theoretical modeling for optoelectronics and nonlinear optics, as well as includes experimental methods, new schemes, new approach and explanation which extends the display technology for laser, semiconductor device technology, medicine, biotechnology, etc. The advanced idea, approach, and information described here will be fruitful for the readers to find a sustainable solution in a fundamental study and in the industry.

**How to reference**

In order to correctly reference this scholarly work, feel free to copy and paste the following:

Youn Jin Kim (2011). Portable LCD Image Quality: Effects of Surround Luminance, Features of Liquid Crystal Display Materials and Processes, Dr. Natalia Kamanina (Ed.), ISBN: 978-953-307-899-1, InTech, Available from: http://www.intechopen.com/books/features-of-liquid-crystal-display-materials-and-processes/portable-lcd-image-quality-effects-of-surround-luminance

# INTECH
open science | open minds